



**HAL**  
open science

## **In silico and in vitro metabolism studies of the new synthetic opiate AP-237 (bucinnazine) using bioinformatics tools**

Romain Pelletier, Alexis Bourdais, Nicolas Fabresse, Pierre-Jean Ferron,,  
Isabelle Morel, Thomas Gicquel, Brendan Le Daré

### ► To cite this version:

Romain Pelletier, Alexis Bourdais, Nicolas Fabresse, Pierre-Jean Ferron,, Isabelle Morel, et al.. In silico and in vitro metabolism studies of the new synthetic opiate AP-237 (bucinnazine) using bioinformatics tools. *Archives of Toxicology*, 2024, 98 (1), pp.165-179. 10.1007/s00204-023-03617-x . hal-04274057

**HAL Id: hal-04274057**

**<https://hal.science/hal-04274057v1>**

Submitted on 11 Jan 2024

**HAL** is a multi-disciplinary open access archive for the deposit and dissemination of scientific research documents, whether they are published or not. The documents may come from teaching and research institutions in France or abroad, or from public or private research centers.

L'archive ouverte pluridisciplinaire **HAL**, est destinée au dépôt et à la diffusion de documents scientifiques de niveau recherche, publiés ou non, émanant des établissements d'enseignement et de recherche français ou étrangers, des laboratoires publics ou privés.

# ***In silico* and *in vitro* metabolism studies of the new synthetic opiate AP-237 (bucinnazine) using bioinformatics tools**

Romain Pelletier<sup>1,2</sup>, Alexis Bourdais<sup>1</sup>, Nicolas Fabresse<sup>3,4</sup>, Pierre-Jean Ferron<sup>1</sup>, Isabelle Morel<sup>1,2</sup>, Thomas Gicquel<sup>1,2</sup>, Brendan Le Daré<sup>1,5</sup>

1. NuMeCan Institute (Nutrition, Metabolisms and Cancer), CHU Rennes, Univ Rennes, INSERM, INRAE, UMR\_A 1341, UMR\_S 1317, F-35000 Rennes, France
2. Rennes University Hospital, Clinical and Forensic Toxicology Laboratory, F-35033 Rennes
3. Laboratory of Pharmacokinetics and Toxicology, La Timone University Hospital, 264 rue Saint Pierre, 13385 Marseille Cedex 5, France
4. Aix Marseille University, INSERM, IRD, SESSTIM, Economic and Social Sciences of Health and Medical Information Processing, Marseille, France
5. Rennes University Hospital, Pharmacy department, F-35033 Rennes, France.

**Corresponding author:** Dr Romain Pelletier (romain.pelletier@chu-rennes.fr)

**Address:** Rennes University Hospital, Clinical and Forensic Toxicology Laboratory, F-35033 Rennes

**Competing interests:** The authors declare no conflict of interest. The funders had no role in the design of the study; in the collection, analyses, or interpretation of data; in the writing of the manuscript, or in the decision to publish the results.

## **Abstract**

The recent emergence of new synthetic opioids (NSOs) compounds in the illicit market is increasingly related to fatal cases. Identification and medical care of NSO intoxication cases are challenging, particularly due to high frequency of new products and extensive metabolism. As the study of NSO metabolism is crucial for the identification of these drugs in cases of intoxication, we aimed to investigate the metabolism of the piperazine NSO AP-237 (=bucinnazine). Two complementary approaches (*in silico* and *in vitro*) were used to identify putative AP-237 metabolites which could be used as consumption markers. *In silico* metabolism studies were realized by combining four open access softwares (MetaTrans, SyGMA, Glory X, Biotransformer 3.0). *In vitro* experiments were performed by incubating AP-237 (20 $\mu$ M) in differentiated HepaRG cells during 0h, 8h, 24h or 48h. Cell supernatant were extracted and analyzed by liquid chromatography coupled to high-resolution mass spectrometry and data were reprocessed using three strategies (MetGem, GNPS or Compound Discoverer®). A total of 28 phase I and six phase II metabolites was predicted *in silico*. Molecular networking identified seven putative phase I metabolites ( $m/z$  203.154,  $m/z$  247.180,  $m/z$  271.180, two  $m/z$  289.191 isomers,  $m/z$  305.186,  $m/z$  329.222) including four previously unknown metabolites. Overall, this cross-disciplinary approach with molecular networking on data acquired *in vitro* and *in silico* prediction enabled to propose relevant candidate as AP-237 consumption markers that could be added to mass spectrometry libraries to help diagnose intoxication.

**Keyword:** NSO, AP-237, bucinnazine, data post-processing strategy

## INTRODUCTION

The opioid overdose crisis is a major public health issue. According to WHO estimates, more than 100,000 deaths are attributed to opioid overdoses each year worldwide (1). At the same time, the recent emergence of new synthetic opioids (NSOs) compounds, often more potent than morphine and mainly illegal, is increasingly related to fatal cases. Since 2009, 57 NSOs (fentanyl derivatives or others) have been detected on Europe's illegal drug market posing concerns regarding their toxicity (2,3). More recently throughout the COVID-19 pandemic, NSOs were the new psychoactive substances (NPS) class most involved in intoxications and fatalities. The total number of single and mixed synthetic opioid cases reported during COVID-19 was 114, with 3 intoxications and 111 fatalities (4).

AP-237 (1-[4-(3-phenyl-2-propen-1-yl)-1-piperazinyl]-1-butanone), also called bucinnazine is a synthetic opioid originally developed as an analgesic drug for which a patent was filled in 1968 (5). While analgesic effect of AP-237 is thought to be approximately 1/3 compared to morphine (6), intravenous administration experiments in rats highlighted a notable reinforcing effect, indicating its dependence potential (7). AP-237 is not currently scheduled in France, but has been detected in the US in the recreational drug supply as well as notified to the EU EWS in May 2019 (8–10). This might be in response to the Chinese inclusion of all fentanyl-related drugs within the list of controlled narcotics (11) leading to a shift towards more varied chemical structures of synthetic opioids. The scientific knowledge regarding AP-237 and its effects in humans is still very limited (8,12). In particular, the lack of metabolic data hinders the identification of consumption markers and thus the obtaining of a representative epidemiological view of consumption data.

The study of NSO metabolism is not always straightforward, due to the scarcity of biological samples and the low availability of standards. As a result, *in vitro* models able to metabolize drugs can be used to study metabolism, including cell-based models such as the HepaRG cell line or human hepatocytes (13–15). Differentiated HepaRG cells (a bipotent cell line capable of differentiating into either cholangiocyte- or hepatocyte-like cells under specific culture conditions) have been described as a robust model for studying both xenobiotics metabolism and toxicity (14,16–18). In particular, this model expresses the majority of the drug processing enzymes including relevant phase I (CYPs (19)) as well as phase II (SULTs (20), and UGTs (20,21)) enzymes and exhibits long-term functional stability whereas human hepatocytes in primary culture lose their drug metabolism ability over time. Because opioid metabolism is predominantly mediated by CYP1A2, CYP2B6, CYP2C8, CYP2C19, CYP2D6 and CYP3A4, the differentiated HepaRG model is a relevant model for studying NSO metabolism (22–24).

Beyond the use of these models to produce metabolites, a powerful analytical apparatus must allow their detection. Thus, innovative bioinformatics approaches have recently been developed to reprocess the complex analytical data acquired during analysis. This includes molecular networking

(MN) which allows untargeted tandem mass spectrometry (MS/MS) data to be organized and represented in a graphical form (25). By analyzing fragmentation spectra, MN makes it possible to gather structurally close molecules in the same sample into a cluster, providing valuable insights into drug biotransformation process (26). MN has already proven its value in the analysis of drug metabolism either *in vitro* or *in vivo* in both clinical or forensic purposes (14,26–28).

Interestingly, the use of *in silico* metabolism prediction software has recently emerged as an interesting alternative to assist metabolite identification (13,29,30). These softwares are mostly convenient, open access, time-saving, and inexpensive tool that help to broaden the metabolite search and confirm data found *in vivo* or *in vitro* (31). In the field of NPS metabolism study, the use of a workflow including *in silico* and *in vitro* studies coupled to LC-HRMS/MS detection tends to be a robust methodology of reference allowing to characterize at best the fate of these substances in the body (13,30,32).

The objective of this study is to assess the AP-237 metabolism using a cross-sectional approach coupling *in silico* and *in vitro* analyses with bioinformatic tools.

## 2. Material and methods

### 2.1. *In silico* metabolite prediction

AP-237 putative metabolites were predicted according to pipeline shown in Figure 1 using AP-237 SMILES string (CCCC(=O)N1CCN(C\C=C\C2=CC=CC=C2)CC1) through the free softwares : GLORYx (33), Biotransformer 3.0 (34), MetaTrans (35) and SyGMa (Systematic Generation of potential Metabolites) (36).

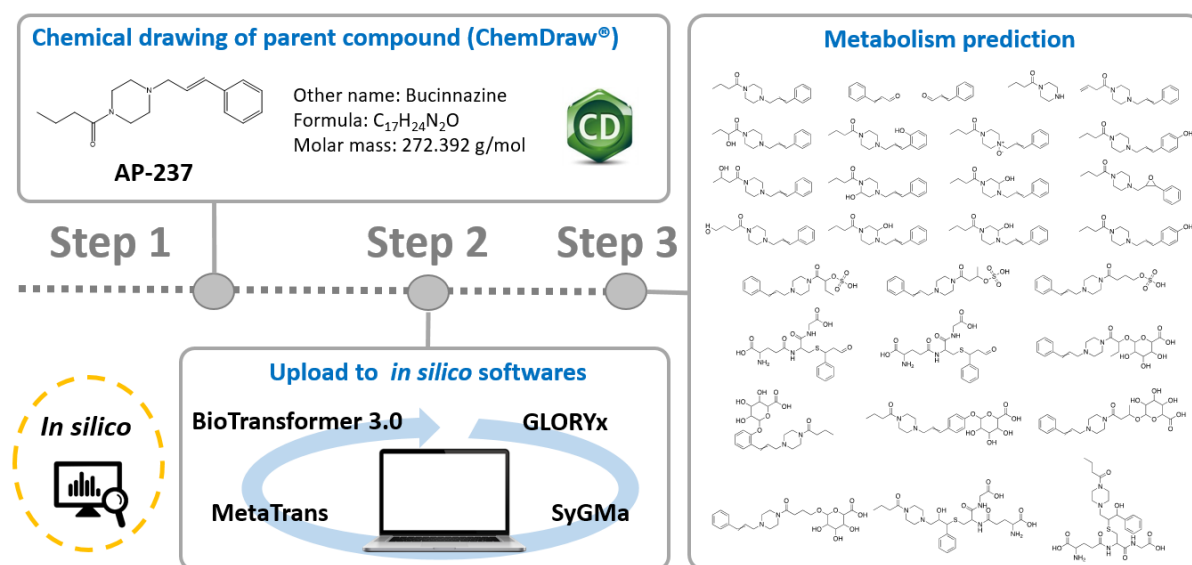


Figure 1. *In silico* methodology to predict AP-237 metabolism using Open access softwares.

Briefly, GLORYx integrates machine learning-based site of metabolism prediction with reaction rule sets to predict and classify the putative structures of metabolites that could be formed by phase I and/or phase II metabolism (33). Biotransformer 3.0 is an open-access software tool that supports the rapid, accurate, and comprehensive prediction of the metabolism of small molecules in both mammals and environmental microorganisms (34). MetaTrans is a rule-free, end-to-end learning-based method for predicting possible human metabolites of small molecules including drugs. The metabolite prediction task is approached as a sequence translation problem with chemical compounds represented using the SMILES notation, and predict metabolites through phase I and phase II drug metabolism as well as other enzymes (35). Sygma is a rule-based method able to predict the potential metabolites of a given parent structure covering a broad range of phase I and phase II metabolism reaction that occur in humans. An empirical probability score is assigned to each rule representing the fraction of correctly predicted metabolites in the training database and covers around 70% of biotransformation reactions (36).

All metabolite structures were generated using ChemDraw software (PerkinElmer, Inc., Waltham, MA, USA) (Figure 1).

## 2.2. *In Vitro* metabolism studies

**Material.** AP-237 was purchased from Cayman chemical company (Ann Arbor, MI, USA). William's E medium (ref: 12551032) was purchased from Gibco (ThermoFischer Scientific, San Jose, CA, USA). Penicillin-streptomycin and glutamine were obtained from Life Technologies (Grand Island, NY, USA). Fetal Bovine Serum (FBS) was purchased from Eurobio (Courtaboeuf, France) and from Hyclone GE Healthcare Life Sciences (Logan, UT, USA). Hydrocortisone hemisuccinate was purchased from Serb (Paris, France). Dimethyl sulfoxide (DMSO), formic acid, and insulin were obtained from Sigma-Aldrich (Saint Louis, GMO, USA).

**Cell culture and treatment.** Progenitor HepaRG cells were cultured as already described (19). Briefly, HepaRG cells were seeded at a density of  $10^5$  cells/well in 96-well plates and cultured in culture medium for two weeks (William's E medium (1X) supplemented with 10% FBS, 50 U/mL penicillin, 50  $\mu$ g/mL streptomycin, 5  $\mu$ g/mL insulin, 2 mM glutamine, 50  $\mu$ M sodium hydrocortisone hemisuccinate and 2% DMSO). Cells were cultured for two more weeks in the same medium supplemented with 2% DMSO to induce cell differentiation into cholangiocyte- and hepatocyte-like cells (19).

Differentiated HepaRG cells were incubated in triplicate with 100  $\mu$ L of AP-237 (20  $\mu$ M) during 0h, 8h, 24h or 48h. The detection of AP-237 and its metabolites was performed using this model as already described (14,29).

## 2.3. LC-HRMS/MS analysis

**Samples extraction.** Cell culture media samples (200  $\mu$ L) were extracted as previously described (30). Briefly, samples were supplemented with 500  $\mu$ L of methanol containing a mix of internal standards at

1 ng/mL (ketamine-D4, promethazine-D8, olanzapine-D8, chlorpromazine-D3, clozapine-D4, flurazepam, risperidone-D4) and then extracted with 300  $\mu$ L of 0.1 M zinc sulfate solution. After supernatant evaporation, the residue was dissolved in 200  $\mu$ L of LC-MS grade water and transferred into chromatographic vials for LC-HR-MS analysis.

### LC-MS settings

Analyses were performed on a Thermo Scientific Q Exactive<sup>TM</sup> (San Jose, USA) mass spectrometer including an Ultimate 3000 RS pump (Thermo Scientific, San Jose, CA, USA). A heated electrospray ionisation-II (HESI-II) ion source was used for the ionization of target compounds. Data acquisition was performed using the Xcalibur<sup>®</sup> 4.3. software (Thermo Scientific).

Non-targeted screening LC-HRMS/MS method used for MN building was performed as already described (29,30). Briefly, liquid chromatography was performed on an Accucore Phenyl Hexyl (100  $\times$  2.1 mm, 2.6  $\mu$ m) (Thermo Scientific, San Jose, CA, USA) at 40 °C using an elution gradient at a flow rate of 500  $\mu$ L/min during 15 min with 10  $\mu$ L as injection volume.

The orbitrap mass spectrometer was operated in positive ESI mode and the acquisition range was 100–700  $m/z$ . Full scan (MS1) data were acquired for each ionization mode at a resolution of 35,000 FWHM, with an AGC target of  $1e6$  and a maximum injection time of 120 ms. Ionic precursor selection was performed in a “data-dependent” mode of operation, where the 5 most intense ions from the previous scan were selected for fragmentation (Top N of 5). MS/MS (MS2) data were acquired at a resolution of 17,500 FWHM with an AGC target of  $1e5$ , maximum injection time was 50 ms and isolation window was 2.0  $m/z$ . The normalized collision energy (NCE) was stepped at 17.5, 35 and 52.5, and the dynamic exclusion time set at 3 s.

### 2.4. Molecular network generation

Spectral data allowed us to generate MN using a semi-quantitative approach. Data acquisition, processing (i.e., MS data conversion, preprocessing, MS1 annotation, and generation of molecular networks), visualization, and network analysis have already been described elsewhere [19]. Briefly, raw data were converted to an open MS format (.mzXML) with ProteoWizard’s MSConvert module (37,38). The mzXML files were then preprocessed using MZmine 3 software (39).

Several steps (deconvolution, deisotoping, FTMS shoulder, alignment, gap-filling) are required to generate MN. The MS1 threshold was chosen at  $10E5$  in order to find all of our internal standards. The single mgf output file was (i) loaded on the Global Natural Products Social networking (GNPS) web-based platform in order to generate the multi-matrix MN (GNPS) or (ii) open with MetGem 1.3.6 software (40).

In GNPS parameters, mass tolerance of precursor and fragment ions used for MS/MS spectral library searching as well as mass tolerance of fragment ions used for MN were set to  $m/z$  0.02. A cosine  $>0.7$

was used for linkage between nodes and the minimum number of common fragment ions shared by two MS/MS spectra was 6. Links between two nodes were kept in the network if each node was in the top 10 most similar nodes.

In MetGem, the minimum cosine score was set to 0.7, the minimum matched peaks was set to 4 and the mass tolerance of fragment ions used for MN was set to  $m/z$  0.02 to allow comparison with data from GNPS. The maximum neighbor number was set to 10 and the maximum connected component size was set to 1000. In t-SNE parameters, the number of iterations, perplexity, learning rate and early exaggeration parameters were respectively set 1000, 6, 200 and 12 according to Olivon et al. (2018) (40).

Molecular networks were visualized using Cytoscape 3.8.0 software (41). SIRIUS software was used to analyzed fragmentation patterns (42). The different steps of the *in vitro* metabolism study approaches are presented in Figure 2.

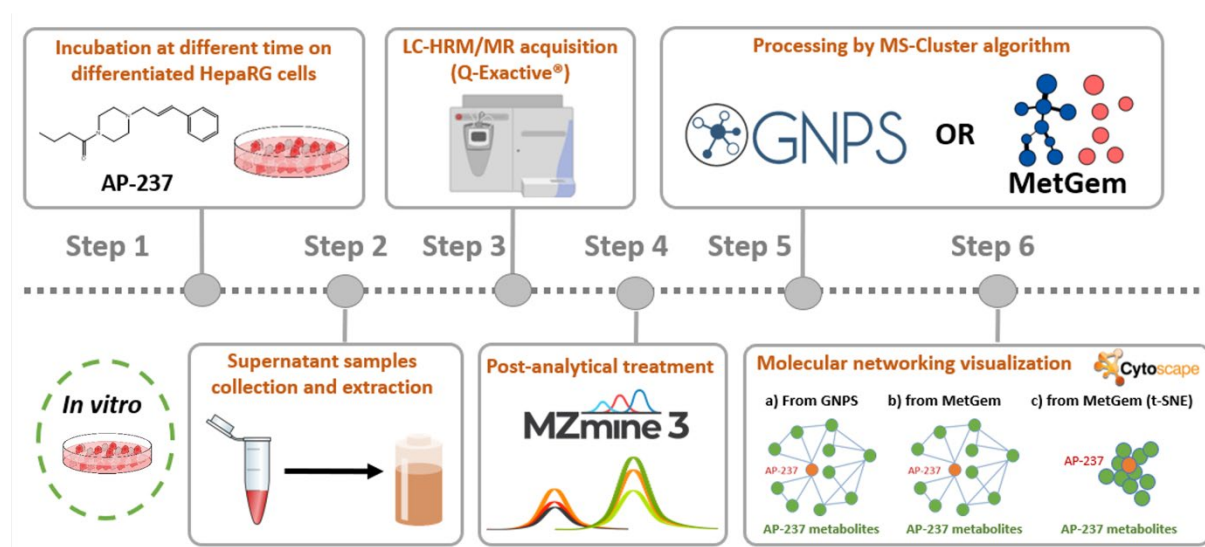


**Figure 2.** Pipeline of the methodology to explore *in vitro* AP-237 metabolism.

## 2.5. Metabolite exploration using Compound Discoverer®

Raw mass spectrometry data were also analyzed using Thermo Scientific Compound Discoverer® (version 3.3.1) to identify metabolites. Phase I and phase II metabolites were generated *in silico* using the .mol file corresponding to AP-237 from Chemspider website. Metabolites were then searched within the four data files based on accurate mass matching (<5ppm) and secondary spectral matching search algorithm. The FISh coverage score was calculated and fragments were auto-annotated with structure, molecular weight, and elemental composition on MS/MS spectra. All features with FISh coverage score  $\geq 50\%$  were filter out to reduce the number of poorly repeatable and unrobust features as already described (43).

### 3. RESULTS

#### 3.1. *In silico* metabolism study of AP-237

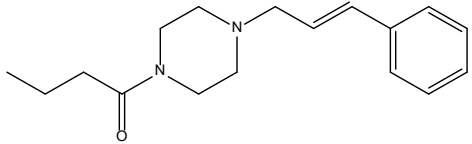
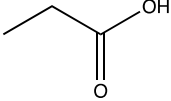
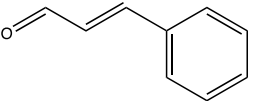
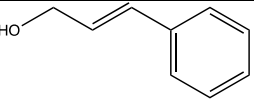
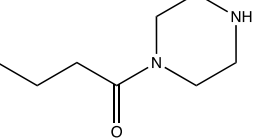
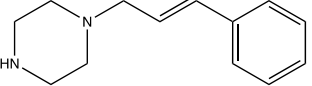
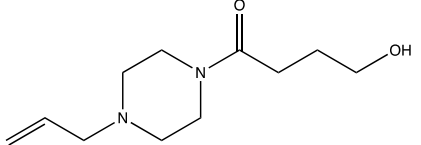
*In silico* prediction of AP-237 metabolism was performed on four different softwares: GloryX, Biotransformer 3.0, MetaTrans and SyGMA. Predicted AP-237 metabolites are synthesized in Table 1 and named P1 to P34. Biotransformation reactions are proposed by SyGMA and Biotransformer 3.0, and the potential enzymes involved are proposed by Biotransformer 3.0. Prediction scores are proposed by GloryX and SyGMA.

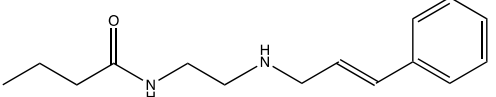
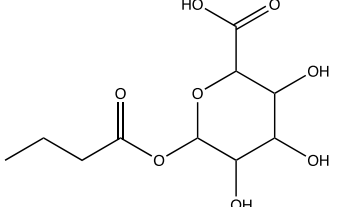
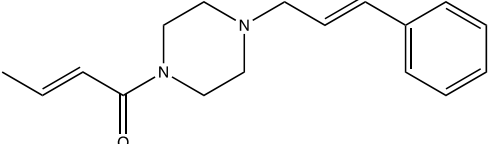
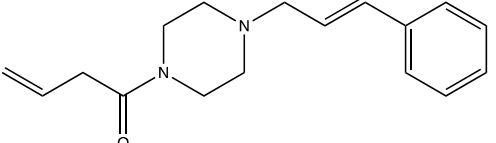
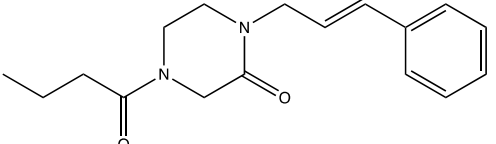
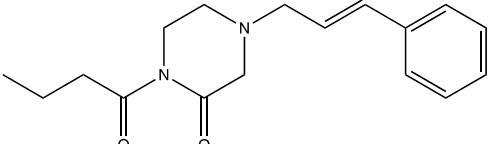
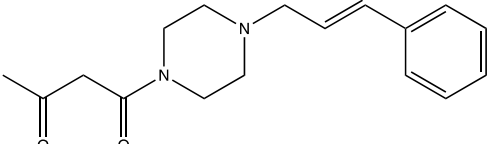
Phase I metabolites included dealkylated (P2 to 4 and P7), desaturated (P10) and oxydated/hydroxylated (P11 to P23, P25 to 27, P30) derivatives mainly produced by CYP1A2, CYP2A6, CYP2B6, CYP2C8, CYP2C9, CYP2C19, CYP2D6 and CYP3A4. Phase II metabolites included sulfoconjugated (P31) and glucuroconjugated (P8, P29, P32 to P34) derivatives. SyGMA was found to predict the most metabolites (n=23) followed by GloryX (n=21), Biotransformer 3.0 (n=13) and MetaTrans (n=9). In particular, SyGMA emerged as the only software predicting Phase II metabolites.

Numerous isomers were proposed by these programs, such as the 14 phase I metabolites with  $m/z$  289.1916, corresponding to the addition of an oxygen atom to the parent molecule. Similarly, 3 glucuroconjugated metabolites are proposed with  $m/z$  465.2237. Taken together, these results show that, excluding isomers, 16 metabolites were proposed.

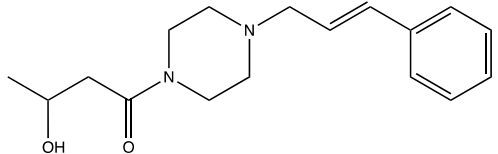
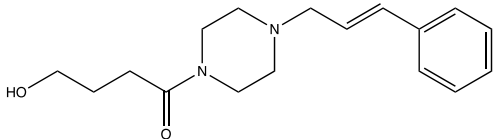
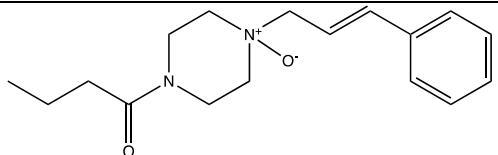
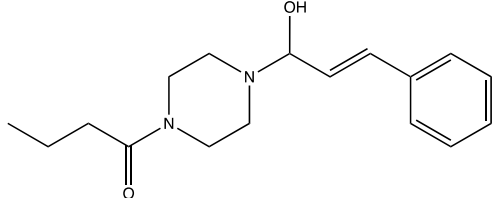
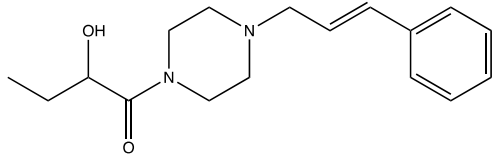
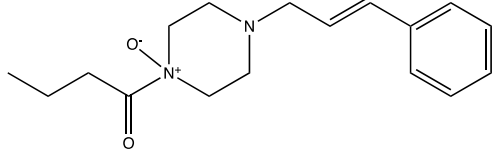


**Table 1. Predicted AP-237 metabolites using four *in silico* metabolism softwares: GloryX (GX), Biotransformer 3.0 (BT3), MetaTrans (MT) and SyGMA (SM).** Using SM, only metabolites with a predicted score > 0.005 are presented. Using GX, only metabolites with a predicted score > 0.1 are presented. "X" indicates that the software has predicted the corresponding metabolite, associated with a probability score (SM and GX) and the biotransformation enzyme (BT3) when available. Chemical structures were generated according to predicted SMILES in softwares.

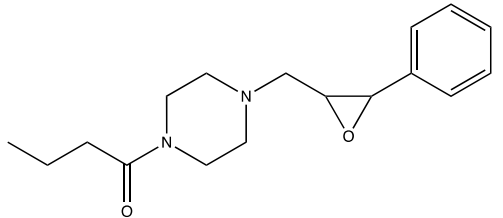
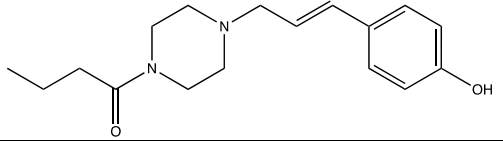
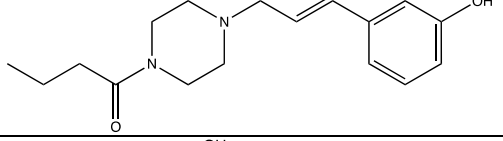
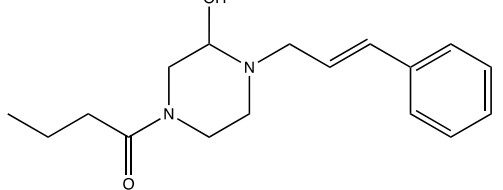
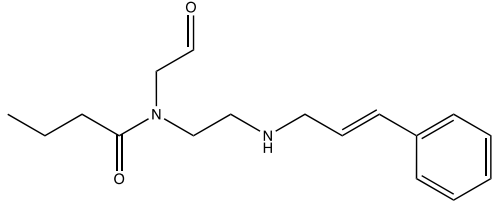
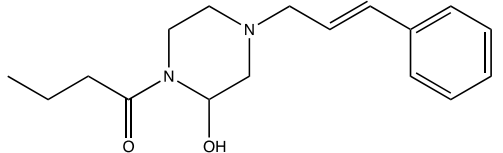
Predicted metabolites	Chemical structure	Formula	$m/z$ [M+H] <sup>+</sup>	Biotransformation	Enzyme	BT3	MT	SM Score	GX Score
Parent (AP-237)		C <sub>17</sub> H <sub>24</sub> N <sub>2</sub> O	273.1967						
P1		C <sub>4</sub> H <sub>8</sub> O <sub>2</sub>	89.0602					X 0.096	X 0.34
P2		C <sub>9</sub> H <sub>8</sub> O	133.0653		CYP1A2, CYP2A6, CYP2B6, CYP2C8, CYP2C9, CYP2C19, CYP2D6, CYP3A4	X	X		X 0.44
P3		C <sub>9</sub> H <sub>10</sub> O	135.0810					X 0.119	
P4		C <sub>8</sub> H <sub>16</sub> N <sub>2</sub> O	157.1341	N-dealkylation	CYP1A2, CYP2A6, CYP2B6, CYP2C8, CYP2C9, CYP2C19, CYP2D6, CYP3A4	X	X	X 0.119	X 0.44
P5		C <sub>13</sub> H <sub>18</sub> N <sub>2</sub>	203.1548	Deacylation				X 0.096	X 0.34
P6		C <sub>11</sub> H <sub>20</sub> N <sub>2</sub> O <sub>2</sub>	213.1603				X		

P7		$C_{15}H_{22}N_2O$	247.1810	di-de-alkylation				X 0.033	X 0.44
P8		$C_{10}H_{16}O_8$	265.0923					X 0.014	
P9		$C_{17}H_{22}N_2O$	271.1810	Desaturation			X		
P10		$C_{17}H_{22}N_2O$	271.1810	Terminal desaturation	CYP1A2, CYP2A6, CYP2C9, CYP2D6, CYP3A4	X			
P11		$C_{17}H_{22}N_2O_2$	287.1759	Oxidation (2 steps)				X 0.048	X 0.16
P12		$C_{17}H_{22}N_2O_2$	287.1759	Oxidation (2 steps)				X 0.048	X 0.12
P13		$C_{17}H_{22}N_2O_2$	287.1759	Oxidation			X		

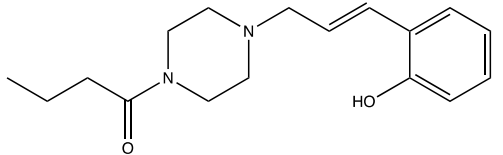
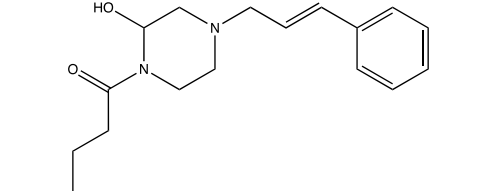
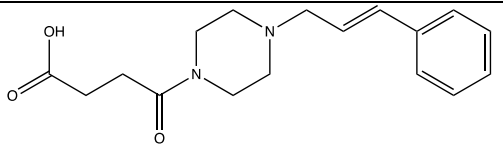
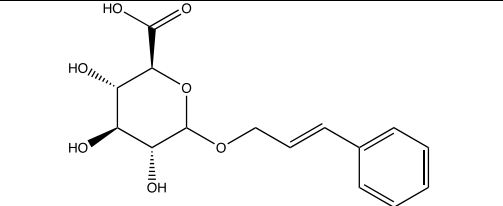
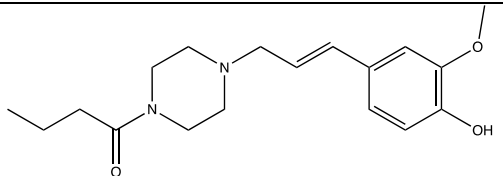
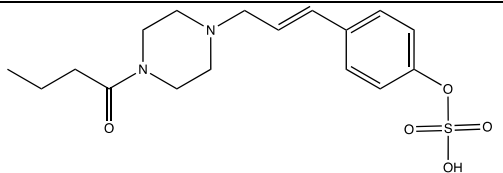
Accepted manuscript

P14		$C_{17}H_{24}N_2O_2$	289.1916	Hydroxylation of penultimate aliphatic secondary carbon	CYP1A2, CYP2A6, CYP2B6, CYP2C8, CYP2C9, CYP2C19, CYP2D6, CYP2E1, CYP3A4	X	X	X 0.106	X 0.44
P15		$C_{17}H_{24}N_2O_2$	289.1916	Hydroxylation of terminal methyl	CYP1A2, CYP2A6, CYP2B6, CYP2C8, CYP2C9, CYP2C19, CYP2D6, CYP2E1, CYP3A4	X	X	X 0.063	X 0.44
P16		$C_{17}H_{24}N_2O_2$	289.1916	N-Oxidation of alicyclic tertiary amine	CYP1A2, CYP2C8, CYP2C19, CYP2D6, CYP3A4	X	X	X 0.06	X 0.44
P17		$C_{17}H_{24}N_2O_2$	289.1916	Aliphatic hydroxylation of carbon alpha to secondary or tertiary alkyl-N	CYP2B6, CYP2C19, CYP2D6	X			X 0.44
P18		$C_{17}H_{24}N_2O_2$	289.1916	Hydroxylation of antepenultimate aliphatic secondary carbon	CYP1A2, CYP2E1	X		X 0.012	X 0.34
P19		$C_{17}H_{24}N_2O_2$	289.1916	N-Oxidation of alicyclic tertiary amine					X 0.34

Accepted manuscript

P20		$C_{17}H_{24}N_2O_2$	289.1916	Epoxidation of alkene	CYP1A2, CYP2B6, CYP2C6, CYP2C8, CYP2C9, CYP2C19, CYP2D6, CYP2E1, CYP3A4	X			X 0.19
P21		$C_{17}H_{24}N_2O_2$	289.1916	Hydroxylation of benzene on carbon para	CYP1A2, CYP2C8, CYP2C9, CYP2C19, CYP2D6, CYP3A4	X	X	X 0.061	X 0.17
P22		$C_{17}H_{24}N_2O_2$	289.1916	Hydroxylation of benzene on carbon meta				X 0.016	X 0.17
P23		$C_{17}H_{24}N_2O_2$	289.1916	Hydroxylation of heterocyclic secondary carbon	CYP1A2, CYP2A6, CYP2C9, CYP2D6, CYP3A4, CYP2B6, CYP2C19	X		X 0.046	X 0.16
P24		$C_{17}H_{24}N_2O_2$	289.1916	Oxidation in ring of the piperazine giving an amina that hydrolyses to aldehyde and amine					X 0.16
P25		$C_{17}H_{24}N_2O_2$	289.1916	Hydroxylation				X 0.046	X 0.12

Accepted manuscript

P26		$C_{17}H_{24}N_2O_2$	289.1916	Hydroxylation of benzene on carbon ortho	CYP1A2, CYP2C8, CYP2C9, CYP2C19, CYP3A4	X			
P27		$C_{17}H_{24}N_2O_2$	289.1916	Hydroxylation of heterocyclic secondary carbon	CYP1A2, CYP2A6, CYP2C9, CYP2D6, CYP3A4	X			
P28		$C_{17}H_{22}N_2O_3$	303.1709	Carboxylation				X 0.030	X 0.44
P29		$C_{15}H_{18}O_7$	311.1131	Glucuronidation				X 0.0120	
P30		$C_{18}H_{26}N_2O_3$	319.2022	Hydroxylation + O-methylation				X 0.021	X 0.17
P31		$C_{17}H_{24}N_2O_5S$	369.1484	Hydroxylation + sulfation				X 0.007	

Accepted manuscript

P32		$C_{23}H_{32}N_2O_8$	465.2237	Glucuronidation				X 0.015	
P33		$C_{23}H_{32}N_2O_8$	465.2237	Glucuronidation				X 0.010	
P34		$C_{23}H_{32}N_2O_8$	465.2237	Glucuronidation				X 0.006	

### 3.2. *In vitro* metabolism study of AP-237 using molecular networking

**Comparison of molecular networking algorithms.** To assess *in vitro* AP-237 metabolite production, differentiated human HepaRG cells were incubated with AP-237 (20 $\mu$ M) for 48h. The cytotoxicity of AP-237 was evaluated and showed no cytotoxic effects (data not shown). Molecular networks using either GNPS or MetGem (classic or t-distributed stochastic neighbor embedding (t-SNE)) were generated from analysis of culture media by LC-HRMS/MS (Table 2, Figure 3). Here, as the t-SNE approach allows nearby spectral features to be grouped together by showing them visually overlapped, it has limitations in terms of data visualization compared to conventional networks created by MetGem or GNPS. To ensure detection of molecules in this data-dependant screening, a mix of 10 internal standards was added before sample extraction. In the entire network, the detection of all internal standards was checked before further analysis.

We showed that GNPS and MetGem found the same number of nodes, but a different number of links, objectifying a different pairing between the compounds. The cosine score was set  $> 0.7$  for cluster matching using GNPS and MetGem. This finding was similar within the AP-237 cluster, where GNPS allowed the inclusion of more compounds within the cluster, associated with a greater number of links between compounds (Table 2).

**Table 2: Comparison of molecular networking procedure after LC-HRMS/MS analysis of culture medium of differentiated HepaRG incubated with AP-237.**

	GNPS	MetGem	
		Classic	t-SNE
Total number of nodes in the molecular network	775	775	775
Total number of links in the molecular network	1419	1167	
Number of nodes in the AP-237 cluster	18	10	10
Number of links in the AP-237 cluster	66	37	

Using GNPS or MetGem classical approach, nodes were labelled in AP-237 clusters with the exact protonated mass ( $m/z$ ) and the links were labelled with the exact mass shift. Nodes were linked together in cluster according to their MS/MS spectral similarities (Figures 3A, C). Using a MetGem t-SNE approach (Figure 3B), the same nodes as MetGem classical approach were identified and pooled together but without visualizing spectral similarities using links.

In terms of analytical data, the GNPS algorithm was able to identify additional compounds in AP-237 cluster (compared with the MetGem algorithm), including in-source fragments (Figure 3C). The cosine scores between compounds were different depending on whether the data were reprocessed by GNPS or MetGem, showing that the 2 tools use different pairing algorithms. However, both tools clustered essentially the same compounds of interest. Only one additional compound ( $m/z$  597.31) was found in

the AP-237 cluster generated by the MetGem algorithm (Figure 3A, B) compared with the GNPS algorithm (Figure 3A). Since MetGem did not provide any superiority over the classic GNPS algorithm, all further post-analytical processing was carried out using the classic GNPS approach.

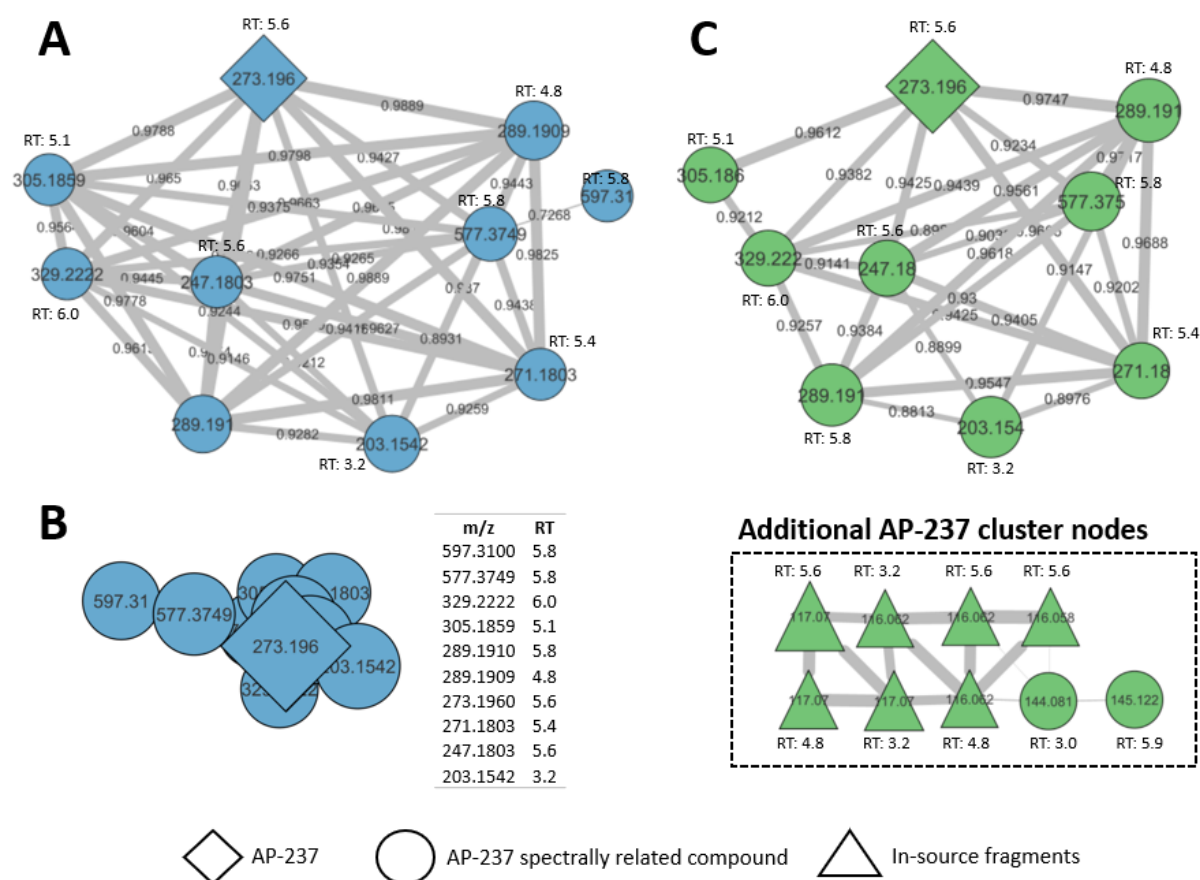


**Figure 3. AP-237 molecular networks after 48h of incubation on differentiated HepaRG cells obtained from A) MetGem generated network, B) t-SNE mode in MetGem and C) GNPS generated molecular network.** The thickness of the links has been set according to the cosine score. Links between AP-237 and "additional AP-237 cluster nodes" have been removed for greater clarity. RT : retention time.

**In vitro AP-237 metabolism kinetic.** In order to explore AP-237 metabolism kinetic, we incubated AP-237 (20  $\mu$ M) in differentiated HepaRG cells during 0h, 8h, 24h or 48h. Culture media analysis at different time allowed us to generate a multi-matrix molecular network which displayed all the MS/MS data acquired during analysis (Figure 4). A specific color was assigned to each time (0h in white, 8h in yellow, 24h in orange and 48h in red). The area of different color in each node represent semi-quantitative concentrations of the corresponding compound in each condition. Visual analysis of the multi-matrix molecular network showed a cluster containing AP-237 linked to other nodes (Figure 4A). First, we found that AP-237 amount decreased over incubation time on the differentiated HepaRG cells. Second, AP-237 was clustered with eight structurally related molecules ( $m/z$  289.191 [RT: 4.8 min and 5.8 min];  $m/z$  305.186 [RT: 5.1 min];  $m/z$  247.180 [RT: 5.6 min];  $m/z$  329.222 [RT: 6.0 min];  $m/z$  271.180 [RT: 5.4 min];  $m/z$  203.154 [RT: 3.2 min];  $m/z$  577.375 [RT: 5.8 min]). Immediately after AP-



237 incubation (0h), none of these latter molecules was detectable. Taken together, these results suggest that these spectrally related molecules are putative AP-237 metabolites.

In this AP-237-containing cluster (Figure 4A), the related putative metabolites could be classified in two subgroups, namely the early metabolites present from 8h of incubation ( $m/z$  289.191 [RT: 4.8 min and 5.8 min];  $m/z$  247.180 [RT: 5.6 min];  $m/z$  329.222 [RT: 6.0 min];  $m/z$  271.180 [RT: 5.4 min];  $m/z$  203.154 [RT: 3.2 min];  $m/z$  577.375 [RT: 5.8 min]) and the late metabolite present from 24h of incubation ( $m/z$  305.186 [RT: 5.1 min]).

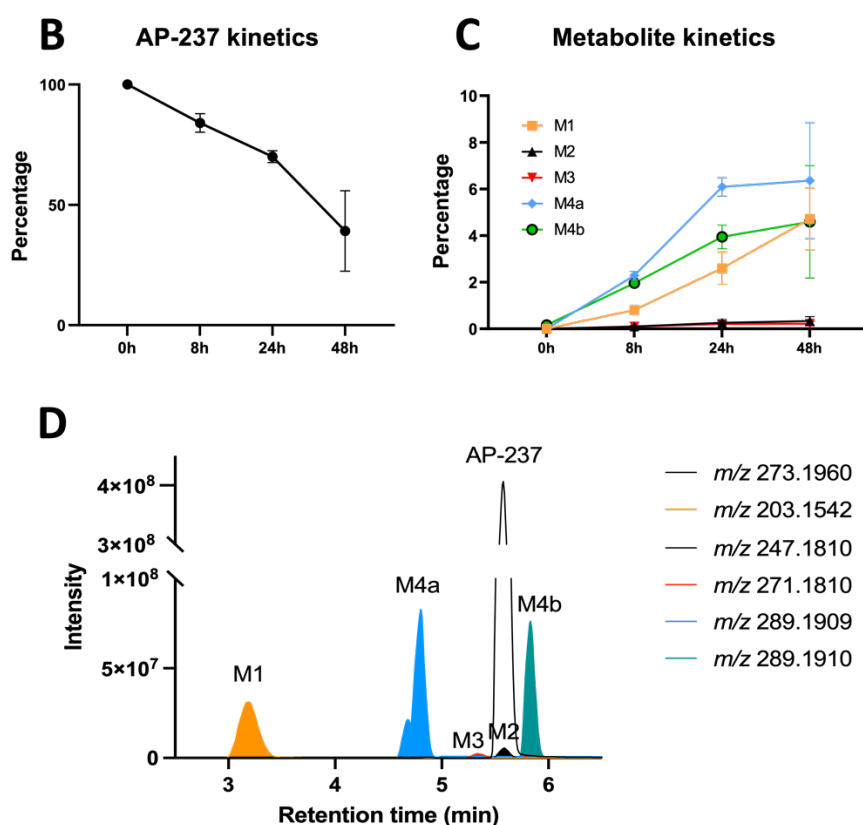
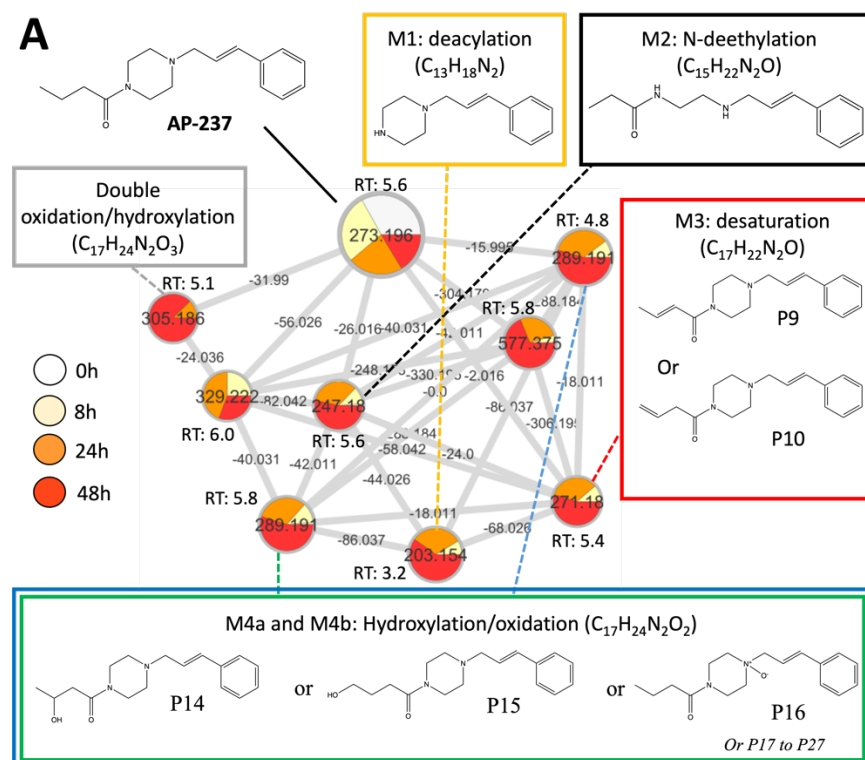


**Figure 4: A) Molecular network and molecule identification. Kinetics study of (B) AP-237 and (C) its main metabolites M1 to M4b in differentiated HepaRG cells supernatants. (D) Reconstituted chromatogram of main metabolites found in one representative *in vitro* experiment after 48h of incubation. Percentage are expressed according to AP-237 peak intensity at 0h (set arbitrary at 100%). The data are quoted as the mean  $\pm$  SEM from experiments performed in triplicate.**

**Identification step.** Information propagation within a molecular network (which consists in determining the structure of an unknown molecule using the structural information of the neighboring nodes) allowed us to propose metabolite identification throughout the AP-237-containing cluster. In particular, mass shifts between spectrally related compounds that could correspond to well-established biotransformation reactions helped us to propose identification as previously described (14,27) (Table S1). The AP-237 fragmentation pattern is displayed in Figure 5, and fragmentation pattern of putative metabolites are presented in supplementary data (Figure S1). Here,  $m/z$  115.054, 117.070 and 91.054 correspond to the main fragments of AP-237 and its metabolites.

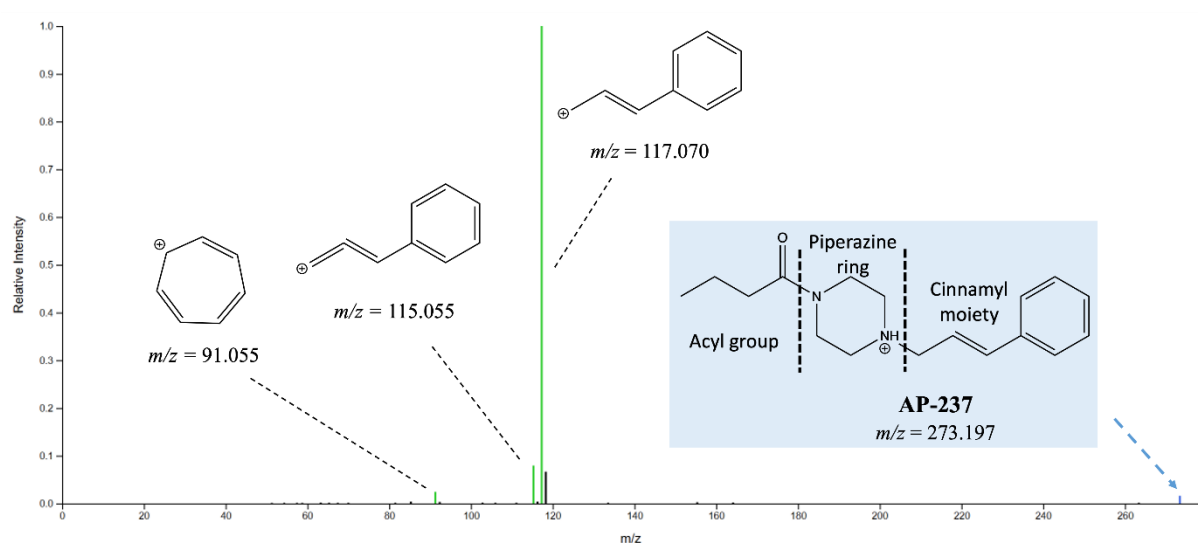


**Figure 5: AP-237 fragmentation pattern in LC-HRMS/MS using SIRIUS Software.** The 91.055 ion (corresponding to the phenyl group of AP-237) is probably rearranged into the more stable tropilium ion.

Our data showed two compounds with the same exact mass ( $m/z$  289.191) but with two different retention time (RT: 4.8 and 5.8 min) (Figure 4A). These nodes were linked to AP-237 ( $m/z$  273.196) with a mass shift of +15.995, corresponding to oxidation/hydroxylation reaction. In the AP-237 cluster, compound  $m/z$  305.186 could correspond to a double oxidation/hydroxylation of AP-237. We also observed mass shifts which could correspond to desaturation (-2.016 Da), giving rise to  $m/z$  271.180. Lastly, a -26.016 Da mass shift which could correspond to N-dealkylation gave rise to  $m/z$  247.180 compound, itself linked to  $m/z$  203.155 compound with a mass shifts of -44.026 Da which could correspond to deacetylation + dehydrogenation. Fragmentation pattern of  $m/z$  577.375 contained a  $m/z$  289.191 fragment suggesting that it could be a dimer of oxidated metabolite ( $[2M+H]^+$ ) (Figure S1). In addition, the same retention time of  $m/z$  577.375 (5.8 min) supported the hypothesis and suggest that it could be a dimer of M4b produced in mass spectrometer. While compound  $m/z$  329.222 was linked to AP-237 with a mass shift of +56.026 which could correspond to the addition of  $C_4H_8$ , we were not able to precisely identify the biotransformation reaction due to a lack of specific fragmentation pattern.

The use of SIRIUS software allowed us to elucidate the fragmentation spectrum of AP-237 and its metabolites, and to propose the  $m/z$  115.0545 and  $m/z$  117.0702 fragments as the most relevant ones for metabolite identification. However, as the fragmentation spectra were not sufficiently rich to deduce where biotransformation reactions took place, the information propagation data were analyzed together with the results of *in silico* analyses to propose the most likely chemical structures of AP-237 metabolites (Figure 4A). These experiments were carried out in triplicate in order to visualize AP-237 metabolism kinetics in conjunction with the appearance of the 5 most intense metabolites identified (Figure 4C).

### **3.3 Comparison to Compound Discoverer®**

In this study, Compound Discoverer® was used to identify AP-237 metabolites and compare the results with metabolites found using open-source software. The metabolites identified by Compound Discoverer® are shown in Table 3 and corresponding mass spectra are presented in supplementary data (Figure S1). Compound Discoverer® identified seven metabolites, three of which were not identified using the molecular networking approach ( $m/z$  307.201,  $m/z$  271.180 (RT 4.7 min) and  $m/z$  369.148). Conversely, the molecular networking approach identified three metabolites not identified by Compound Discoverer® ( $m/z$  203.154,  $m/z$  247.180 and  $m/z$  329.222).

**Table 3: AP-237 metabolites identified by Compound Discoverer® after incubation of AP-237 on HepaRG cells for 8h, 24h and 48h.** To reduce the number of poorly repeatable and unrobust features, compounds with FISh coverage score  $\geq 50\%$  were filter out.

<b>I</b>	<b>Formula</b>	<b>RT (min)</b>	<b>Transformations</b>	<b>Composition Change</b>	<b>FISh Coverage (%)</b>	<b>8h</b>	<b>24h</b>	<b>48h</b>
<b>271.180</b>	$C_{17}H_{22}N_2O$	5.9	Desaturation	-(H <sub>2</sub> )	71.05	X	X	X
<b>271.180</b>	$C_{17}H_{22}N_2O$	4.7	Desaturation	-(H <sub>2</sub> )	73.68	X	X	X
<b>289.191</b>	$C_{17}H_{24}N_2O_2$	5.8	Oxidation	+(O)	63.64	X	X	X
<b>289.191</b>	$C_{17}H_{24}N_2O_2$	4.7	Oxidation	+(O)	58.14	X	X	X
<b>305.186</b>	$C_{17}H_{24}N_2O_3$	5.1	Oxidation, Oxidation	+(O <sub>2</sub> )	100			X
<b>307.201</b>	$C_{17}H_{26}N_2O_3$	4.4	Hydration, Oxidation	+(H <sub>2</sub> O <sub>2</sub> )	67.74		X	X
<b>369.148</b>	$C_{17}H_{24}N_2O_5S$	4.5	Oxidation, Sulfation	+(O <sub>4</sub> S)	71.43			X

On the basis of *in vitro* and *in silico* analyses, Table 4 summarizes the characteristics of the metabolites proposed as the most relevant to add to mass spectrometry databases. This aims to increase the probability of detecting intoxication in humans.

**Table 4: Synthesis List of AP-237 relevant metabolites obtained in *in vitro* experiments.** RT: retention time

Name	Formula	RT (min)	[M+H] <sup>+</sup> observed	[M+H] <sup>+</sup> expected	Δppm	Main observed fragment ions	Delta m/z compared with AP-237	Biotransformation reactions
AP-237 (Parent)	C <sub>17</sub> H <sub>24</sub> N <sub>2</sub> O	5.5	273.1960	273.1967	-2.56	117.0702 115.0545 91.0548	NA	NA
M1	C <sub>13</sub> H <sub>18</sub> N <sub>2</sub>	3.1	203.1542	203.1548	-2.95	117.0702 115.0545 91.0548	-70.042	Deacylation
M2	C <sub>15</sub> H <sub>22</sub> N <sub>2</sub> O	5.6	247.1803	247.1810	-2.83	117.0702 115.0545 91.0548	-26.016	N-deethylation
M3	C <sub>17</sub> H <sub>22</sub> N <sub>2</sub> O	5.3	271.1803	271.1810	-2.58	117.0702 115.0545 91.0548	-2.016	Desaturation
M4a	C <sub>17</sub> H <sub>24</sub> N <sub>2</sub> O <sub>2</sub>	4.8	289.1909	289.1916	-2.58	117.0702 115.0545 91.0548	15.995	Oxidation / hydroxylation
M4b	C <sub>17</sub> H <sub>24</sub> N <sub>2</sub> O <sub>2</sub>	5.8	289.1910	289.1916	-2.07	117.0702 115.0545 91.0548	15.995	

#### 4. DISCUSSION

In this study, we aimed to investigate the AP-237 metabolism using a cross-sectional approach coupling *in silico* and *in vitro* analyses coupled to bioinformatic tools. In the absence of *in vivo* intoxication cases, exploring metabolism using these approaches can provide potentially useful consumption markers for the future identification of intoxication in humans.

The *in silico* metabolism study approach makes it possible to propose metabolite structures associated with biotransformation reactions, and potentially the enzymes involved, as well as a prediction score. By cross-referencing the information obtained by different prediction software programs, we increase the probability of obtaining reliable, predictive information on phenomena that can be observed *in vitro* or *in vivo*. This approach has already been used to explore the metabolism of new drug candidates (29) or NPS (13,30,32). Here we have combined four *in silico* software packages to predict the metabolism of the NSO AP-237.

The GloryX and SygMA software packages are interesting by adding a prediction score to the results, enabling the relevance of the proposed metabolites to be stratified (33,36). Biotransformer 3.0 also proposed numerous potential enzymes involved in biotransformation reactions. Here, AP-237 metabolism was predicted to be predominantly carried out by phase I enzymes, which is consistent with the overall results reported by the four software packages. Although MetaTrans doesn't offer metabolic pathway prediction features superior to the other software tested in this study, it has enabled us to cross-reference information with the aim of gaining a better understanding of their reliability. Interestingly, the predicted *m/z* data can be incremented in the LC-HRMS/MS inclusion list for the purpose of semi-targeted screening as previously described (32,44,45).

In terms of limitations, the predicted metabolites do not always seem relevant (as exemplified by P26 which is very unlikely since most often less hindered carbons are more accessible), sometimes with redundancies. In addition, obvious metabolites were not predicted such as aldehyde or alcohol metabolites. Concerning the predicted metabolite P24, it can be assumed that it is preceded by the formation of an iminium metabolite as described by Kalgutkar *et al.* (2020) (46). Although this reactive intermediary metabolite can be trapped by cyanide to form stable adducts, we can't rule out their involvement in toxicity phenomena through the formation of protein and DNA adducts (46). Consequently, *in silico* solution interest seems to remain restricted for now on assisting metabolite predictions using *in vitro* models, and *in silico* results should be treated with caution. Also, in the case of isomer prediction, these approaches cannot predict chromatographic retention times, which limits the use of results in comparison with *in vitro* or *in vivo* analytical data. Since fragmentation patterns of AP-237 and its metabolites lack of specificity, chromatographic separation would appear to be an important additional criterion for their identification. Overall, in the absence of reliable NPS-specific software, the



combination of several *in silico* approaches seems interesting. These conclusions need to be confirmed with other molecules, in particular NSOs, and compared with analytical data to assess their relevance.

*In vitro*, the differentiated HepaRG model has already shown its relevance in the study of xenobiotic metabolism, including NPS (30,47,48). In this study, we confirm its relevance to the study of NSO metabolism.

A total of nine putative phase I metabolites were proposed *in vitro*, including six previously unknown metabolites ( $m/z$  305.186 [RT: 5.1 min];  $m/z$  247.180 [RT: 5.6 min];  $m/z$  329.222 [RT: 6.0 min];  $m/z$  271.180 [RT: 5.4 min];  $m/z$  271.180 [RT 4.7 min];  $m/z$  307.201 [RT: 4.4 min]). Only one phase II metabolites ( $m/z$  369.148) was found after 48h incubation using Compound Discoverer, despite SyGMA Software prediction. Given that the differentiated HepaRG model is capable of producing phase II metabolites, these data need to be confirmed *in vivo*, in particular in urine or bile samples. The kinetic study of metabolism provides us with valuable data on the nodes linked to AP-237. Indeed, by visualizing the clearance of AP-237, correlated with the appearance of spectrally related molecules, we present strong evidence that these are metabolites. As their early and late metabolite profiles could be distinguished, a better understanding of the metabolic dynamics can be proposed. The AP-237 fragmentation pattern displayed characteristic fragments at  $m/z$  115.0545 and 117.0702 corresponding to the cinnamyl moiety. In the literature, studies on AP-237 metabolism in rats, rabbits and guinea pigs identified seven metabolites, namely hydroxylated AP-237 ( $m/z$  289.1916), 1-cinnamylpiperazine ( $m/z$  203.1548), 1-(4-hydroxycinnamyl)piperazine ( $m/z$  219.1497), benzoic acid ( $m/z$  123.0446), 4-hydroxybenzoic acid ( $m/z$  139.0395), hippuric acid ( $m/z$  180.0660) and 4-hydroxyhippuric acid ( $m/z$  196.0609) (12,49,50).

These results are also consistent with most piperazine metabolism data which display extensive phase I metabolism including CYP3A4-dependent N-dealkylation and CYP2D6-dependent oxidation to hydroxylates (51). These two cytochromes were proposed by Biotransformer 3 software. In particular, metabolism studies on 2-methyl-AP-237 identified 4 hydroxylated metabolites in which hydroxylation occurred mainly on the piperazine moiety and to a lesser extent on the cinnamyl moiety (52–54). Similarly on AP-238 compound, 27 phase I metabolites and five phase II metabolites were identified through liquid chromatography-quadrupole time-of-flight mass spectrometry in *in vitro* and *in vivo* (human urine sample) assay. The main *in vivo* metabolites were built by hydroxylation combined with further metabolic reactions such as O-methylation or N-deacylation (55). Lastly, MT-45 metabolism study (another piperazine derivative synthetic opioid sharing same structural similarities with AP-237) found low proportion of phase II metabolites, supporting the idea of a rather weak phase II metabolism for these compounds (56).

The commercial Compound Discoverer® software proved as effective as the open access software in identifying the main metabolites of AP-237. However, its use proved less flexible than open access

solutions, due to the impossibility of modifying all data filter parameters and license fees may also be an obstacle to its use by some laboratories. In terms of the open source algorithm used for molecular networking, MetGem and GNPS proved equivalent for the identification of the main metabolites of AP-237, although the t-SNE representation was difficult to read. Consequently, both approaches can be used according to researcher's expertise. The main limitation in identifying metabolites was knowing the location of biotransformation reactions due to poor fragmentation spectra. For this reason, we feel it would be useful to obtain metabolite standards when available, or to have them synthesized in order to increase confidence in the structure of the proposed metabolites. This would enable to compare retention times and MS2 spectra.

Overall, the combined use of different *in silico* and *in vitro* models coupled with the molecular network approach allows us to gain confidence in our proposals for potential consumption markers.

## 5. CONCLUSION

*In vitro* AP-237 metabolism study on differentiated HepaRG cells supported by *in silico* prediction using four complementary software allowed to identify seven AP-237 metabolites among which four were previously unknown. Biotransformation reactions seem to occur mainly by oxidation/hydroxylation on the acyl/piperazine moiety. Given their detection intensity in *in vitro* samples, we propose compounds  $m/z$  203.1548,  $m/z$  247.1810,  $m/z$  271.1810 and  $m/z$  289.1916 as markers of AP-237 consumption. These compounds can therefore reasonably be added to mass spectrometry libraries to help diagnose intoxication, notably by increasing the detection window.

## REFERENCES

1. United Nations Office on Drugs and Crime. Drug market trends: cannabis, opioids [Internet]. 2021. Available from: [https://www.unodc.org/res/wdr2021/field/WDR21\\_Booklet\\_3.pdf](https://www.unodc.org/res/wdr2021/field/WDR21_Booklet_3.pdf)
2. Observatoire européen des drogues et des toxicomanies, editor. European drug report: trends and developments. Luxembourg: Publications office of the European Union; 2020.
3. Blanckaert P, Cannaert A, Van Uytvanghe K, Hulpia F, Deconinck E, Van Calenbergh S, et al. Report on a novel emerging class of highly potent benzimidazole NPS opioids: Chemical and in vitro functional characterization of isotonitazene. *Drug Test Anal.* 2020 Apr;12(4):422–30.
4. Lo Faro AF, Berardinelli D, Cassano T, Dendramis G, Montanari E, Montana A, et al. New Psychoactive Substances Intoxications and Fatalities during the COVID-19 Epidemic. *Biology.* 2023 Feb 8;12(2):273.
5. Carrano RA, Kimura KK, McCurdy DH. Analgesic and tolerance studies with AP-237, a new analgesic. *Arch Int Pharmacodyn Ther.* 1975 Jan;213(1):41–57.
6. Ping Y, Jing C, Qing J. Comparison of the use of different analgesics in the course of anesthesia care based on pharmacoeconomics. *Pak J Pharm Sci.* 2018 Sep;31(5(Special)):2241–7.
7. Experimental study on dependence-producing properties of Qiang Tong Ding (AP-237). | CiNii Research [Internet]. [cited 2023 May 10]. Available from: <https://cir.nii.ac.jp/crid/1571417124541832064>
8. Fogarty MF, Vandeputte MM, Krotulski AJ, Papsun D, Walton SE, Stove CP, et al. Toxicological and pharmacological characterization of novel cinnamylpiperazine synthetic opioids in humans and in vitro including 2-methyl AP-237 and AP-238. *Arch Toxicol.* 2022 Jun;96(6):1701–10.
9. UNODC. Early Warning Advisory (EWA) on New Psychoactive Substances (NPS) [Internet]. 2023. Available from: <https://www.unodc.org/LSS/Home/NPS>
10. WHO Expert Committee on Drug Dependence. Critical review report: 2-Methyl AP-237 [Internet]. 2022. Available from: [https://cdn.who.int/media/docs/default-source/controlled-substances/45th-ecdd/2-methyl-ap-237\\_draft.pdf?sfvrsn=768c7c03\\_1](https://cdn.who.int/media/docs/default-source/controlled-substances/45th-ecdd/2-methyl-ap-237_draft.pdf?sfvrsn=768c7c03_1)
11. News: April 2019 – China: Announcement to place all fentanyl-related substances under national control [Internet]. [cited 2023 May 10]. Available from: <https://www.unodc.org/LSS/announcement/Details/f2adea68-fbed-4292-a4cc-63771c943318>
12. Resnik K, Brandão P, Alves EA. DARK Classics in Chemical Neuroscience: Bucinnazine. *ACS Chem Neurosci.* 2021 Oct 6;12(19):3527–34.
13. Di Trana A, Brunetti P, Giorgetti R, Marinelli E, Zaami S, Busardò FP, et al. In silico prediction, LC-HRMS/MS analysis, and targeted/untargeted data-mining workflow for the profiling of phenylfentanyl in vitro metabolites. *Talanta.* 2021 Dec;235:122740.
14. Le Daré B, Ferron PJ, Allard PM, Clément B, Morel I, Gicquel T. New insights into quetiapine metabolism using molecular networking. *Sci Rep.* 2020 Dec;10(1):19921.
15. Ferron PJ, Le Daré B, Bronsard J, Steichen C, Babina E, Pelletier R, et al. Molecular Networking for Drug Toxicities Studies: The Case of Hydroxychloroquine in COVID-19 Patients. *IJMS.* 2021 Dec 22;23(1):82.

16. Cerec V, Glaise D, Garnier D, Morosan S, Turlin B, Drenou B, et al. Transdifferentiation of hepatocyte-like cells from the human hepatoma HepaRG cell line through bipotent progenitor. *Hepatology*. 2007 Apr;45(4):957–67.
17. Guguen-Guillouzo C, Guillouzo A. Setup and Use of HepaRG Cells in Cholestasis Research. In: Vinken M, editor. *Experimental Cholestasis Research* [Internet]. New York, NY: Springer New York; 2019 [cited 2022 May 26]. p. 291–312. (Methods in Molecular Biology; vol. 1981). Available from: [http://link.springer.com/10.1007/978-1-4939-9420-5\\_19](http://link.springer.com/10.1007/978-1-4939-9420-5_19)
18. Guillouzo A, Corlu A, Aninat C, Glaise D, Morel F, Guguen-Guillouzo C. The human hepatoma HepaRG cells: A highly differentiated model for studies of liver metabolism and toxicity of xenobiotics. *Chemico-Biological Interactions*. 2007 May;168(1):66–73.
19. Aninat C, Piton A, Glaise D, Le Charpentier T, Langouët S, Morel F, et al. Expression of cytochromes P450, conjugating enzymes and nuclear receptors in human hepatoma HepaRG cells. *Drug Metab Dispos*. 2006 Jan;34(1):75–83.
20. Hugbart C, Verres Y, Le Daré B, Bucher S, Vène E, Bodin A, et al. Non-oxidative ethanol metabolism in human hepatic cells in vitro: Involvement of uridine diphosphoglucuronosyltransferase 1A9 in ethylglucuronide production. *Toxicology in Vitro*. 2020 Aug;66:104842.
21. Quesnot N, Bucher S, Gade C, Vlach M, Vene E, Valença S, et al. Production of chlorzoxazone glucuronides via cytochrome P4502E1 dependent and independent pathways in human hepatocytes. *Archives of Toxicology*. 2018 Oct;92(10):3077–91.
22. Smith HS. Opioid Metabolism. *Mayo Clinic Proceedings*. 2009 Jul;84(7):613–24.
23. Pérez-Mañá C, Papaseit E, Fonseca F, Farré A, Torrens M, Farré M. Drug Interactions With New Synthetic Opioids. *Front Pharmacol*. 2018 Oct 11;9:1145.
24. Rojek S, Poljańska E, Chaim W, Maciów-Głąb M, Bystrowska B. Metabolic Evaluation of Synthetic Opioids on the Example of U-47700 with the Use of In Vitro and In Vivo Methods for Forensic Toxicology Application. *Toxics*. 2023 Feb 25;11(3):220.
25. Wang M, Carver JJ, Phelan VV, Sanchez LM, Garg N, Peng Y, et al. Sharing and community curation of mass spectrometry data with Global Natural Products Social Molecular Networking. *Nature Biotechnology*. 2016 Aug;34(8):828–37.
26. Allard S, Allard P, Morel I, Gicquel T. Application of a molecular networking approach for clinical and forensic toxicology exemplified in three cases involving 3-MeO-PCP, doxylamine, and chlormequat. *Drug Test Anal*. 2019 May;11(5):669–77.
27. Le Daré B, Allard S, Bouvet R, Baert A, Allard PM, Morel I, et al. A case of fatal acebutolol poisoning: an illustration of the potential of molecular networking. *International Journal of Legal Medicine* [Internet]. 2019 Apr 17 [cited 2019 Jun 28]; Available from: <http://link.springer.com/10.1007/s00414-019-02062-9>
28. Le Daré B, Ferron PJ, Couette A, Ribault C, Morel I, Gicquel T. In vivo and in vitro  $\alpha$ -amanitin metabolism studies using molecular networking. *Toxicology Letters*. 2021 Aug;346:1–6.
29. Pelletier R, Gicquel T, Simoes Eugenio M, Ferron PJ, Morel I, Delehouzé C, et al. A Transversal Approach Combining In Silico, In Vitro and In Vivo Models to Describe the Metabolism of the Receptor Interacting Protein 1 Kinase Inhibitor Sibiriline. *Pharmaceutics*. 2022 Nov 30;14(12):2665.

30. Pelletier R, Le Daré B, Ferron PJ, Le Bouëdec D, Kernalléguen A, Morel I, et al. Use of innovative, cross-disciplinary in vitro, in silico and in vivo approaches to characterize the metabolism of chloro-alpha-pyrrolidinovalerophenone (4-Cl-PVP). *Arch Toxicol* [Internet]. 2022 Dec 5 [cited 2023 Feb 17]; Available from: <https://link.springer.com/10.1007/s00204-022-03427-7>
31. Kirchmair J, Göller AH, Lang D, Kunze J, Testa B, Wilson ID, et al. Predicting drug metabolism: experiment and/or computation? *Nat Rev Drug Discov*. 2015 Jun;14(6):387–404.
32. Malaca S, Busardò FP, Giorgetti R, Huestis MA, Carlier J. In silico prediction, human hepatocyte metabolism, LC-HRMS/MS analysis, and targeted/nontargeted data-mining to characterize 4-acetoxy-N,N-diisopropyl-tryptamine metabolism. *Toxicologie Analytique et Clinique*. 2022 Sep;34(3):S135–6.
33. de Bruyn Kops C, Šicho M, Mazzolari A, Kirchmair J. GLORYx: Prediction of the Metabolites Resulting from Phase 1 and Phase 2 Biotransformations of Xenobiotics. *Chem Res Toxicol*. 2021 Feb 15;34(2):286–99.
34. Djoumbou-Feunang Y, Fiamoncini J, Gil-de-la-Fuente A, Greiner R, Manach C, Wishart DS. BioTransformer: a comprehensive computational tool for small molecule metabolism prediction and metabolite identification. *J Cheminform*. 2019 Dec;11(1):2.
35. Litsa EE, Das P, Kaviraki LE. Prediction of drug metabolites using neural machine translation. *Chem Sci*. 2020;11(47):12777–88.
36. Ridder L, Wagener M. SyGMa: Combining Expert Knowledge and Empirical Scoring in the Prediction of Metabolites. *ChemMedChem*. 2008 May 19;3(5):821–32.
37. Holman JD, Tabb DL, Mallick P. Employing ProteoWizard to Convert Raw Mass Spectrometry Data. *CP in Bioinformatics* [Internet]. 2014 Jun [cited 2023 Apr 5];46(1). Available from: <https://onlinelibrary.wiley.com/doi/10.1002/0471250953.bi1324s46>
38. Kessner D, Chambers M, Burke R, Agus D, Mallick P. ProteoWizard: open source software for rapid proteomics tools development. *Bioinformatics*. 2008 Nov 1;24(21):2534–6.
39. Schmid R, Heuckeroth S, Korf A, Smirnov A, Myers O, Dyrland TS, et al. Integrative analysis of multimodal mass spectrometry data in MZmine 3. *Nat Biotechnol* [Internet]. 2023 Mar 1 [cited 2023 Apr 6]; Available from: <https://www.nature.com/articles/s41587-023-01690-2>
40. Olivon F, Elie N, Grelier G, Roussi F, Litaudon M, Touboul D. MetGem Software for the Generation of Molecular Networks Based on the t-SNE Algorithm. *Anal Chem*. 2018 Dec 4;90(23):13900–8.
41. Shannon P. Cytoscape: A Software Environment for Integrated Models of Biomolecular Interaction Networks. *Genome Research*. 2003 Nov 1;13(11):2498–504.
42. Dührkop K, Fleischauer M, Ludwig M, Aksenov AA, Melnik AV, Meusel M, et al. SIRIUS 4: a rapid tool for turning tandem mass spectra into metabolite structure information. *Nature Methods*. 2019 Apr;16(4):299–302.
43. Wang X, Chang X, Luo X, Su M, Xu R, Chen J, et al. An Integrated Approach to Characterize Intestinal Metabolites of Four Phenylethanoid Glycosides and Intestinal Microbe-Mediated Antioxidant Activity Evaluation In Vitro Using UHPLC-Q-Exactive High-Resolution Mass Spectrometry and a 1,1-Diphenyl-2-picrylhydrazyl-Based Assay. *Front Pharmacol*. 2019 Jul 25;10:826.

44. Busardò FP, Lo Faro AF, Sirignano A, Giorgetti R, Carlier J. In silico, in vitro, and in vivo human metabolism of acetazolamide, a carbonic anhydrase inhibitor and common “diuretic and masking agent” in doping. *Arch Toxicol*. 2022 Jul;96(7):1989–2001.
45. Carlier J, Berardinelli D, Montanari E, Sirignano A, Di Trana A, Busardò FP. 3F- $\alpha$ -pyrrolydinovalerophenone (3F- $\alpha$ -PVP) in vitro human metabolism: Multiple in silico predictions to assist in LC-HRMS/MS analysis and targeted/untargeted data mining. *Journal of Chromatography B*. 2022 Mar;1193:123162.
46. Kalgutkar AS, Driscoll JP. Is there enough evidence to classify cycloalkyl amine substituents as structural alerts? *Biochemical Pharmacology*. 2020 Apr;174:113796.
47. Gicquel T, Pelletier R, Richeval C, Gish A, Hakim F, Ferron P, et al. Metabolite elucidation of 2-fluoro-deschloroketamine (2F-DCK) using molecular networking across three complementary *in vitro* and *in vivo* models. *Drug Test Anal*. 2021 Sep 20;:3162.
48. Pelletier R, Le Daré B, Grandin L, Couette A, Ferron PJ, Morel I, et al. New psychoactive substance cocktail in an intensive care intoxication case elucidated by molecular networking. *Clinical Toxicology*. 2021 Jun 4;:1–4.
49. Baba S, Morishita S. Studies on drug metabolism by use of isotopes. XVI. Species differences in metabolism of 1-butyryl-4-cinnamylpiperazine hydrochloride. *Chem Pharm Bull*. 1975;23(9):1949–54.
50. Morishita SI, Baba S, Nagase Y. Studies on Drug Metabolism by Use of Isotopes XX: Ion Cluster Technique for Detection of Urinary Metabolites of 1-Butyryl-4-cinnamylpiperazine by Mass Chromatography. *Journal of Pharmaceutical Sciences*. 1978 Jun;67(6):757–61.
51. Silvio Caccia. N-Dealkylation of Arylpiperazine Derivatives: Disposition and Metabolism of the 1-Aryl-Piperazines Formed. *CDM*. 2007 Aug 1;8(6):612–22.
52. Hassanien S, Layle N, Holt M, Zhao T, Lula D. 2-methyl AP-237. Cayman NPS metabolism monograph [Internet]. 2023. Available from: <https://www.caymanchem.com/product/26485>
53. Samano K, Clouette R, Peterson DC. Fatality from 2-methyl AP-237 (2-methyl buccinazine), a novel synthetic opioid drug gaining recreational popularity. 2021. (Proceedings of the 2021 Society of Forensic Toxicologists Annual Meeting).
54. Truver MT, Crosby MM, Gillette AT, Brogan SC, Hoyer JL, Chronister CW, et al. Fatal intoxication involving 2-methyl AP -237. *Journal of Forensic Sciences*. 2023 Jul;68(4):1419–24.
55. Brunetti P, Berardinelli D, Giorgetti A, Schwelm HM, Haschimi B, Pelotti S, et al. Human metabolism and basic pharmacokinetic evaluation of AP-238: A recently emerged acylpiperazine opioid. *Drug Testing and Analysis*. 2023 Jun 27;:3535.
56. McKenzie C, Sutcliffe OB, Read KD, Scullion P, Epemolu O, Fletcher D, et al. Chemical synthesis, characterisation and in vitro and in vivo metabolism of the synthetic opioid MT-45 and its newly identified fluorinated analogue 2F-MT-45 with metabolite confirmation in urine samples from known drug users. *Forensic Toxicol*. 2018 Jul;36(2):359–74.

## SUPPLEMENTARY FIGURE AND TABLES LEGENDS

**Figure S1: (A-E) Fragmentation spectrum of the most likely AP-237 metabolites. The spectra on the left were visualized using SIRIUS software, while the spectra on the right were visualized and annotated automatically using Compound Discoverer® software. (F-H) Fragmentation spectrum of compounds present in the molecular network but not proposed by Compound Discoverer®.**

**Table S1: Main biotransformation reactions found in AP-237 *in vitro* experiments with associated loss of mass or gain of mass for the parent molecule.**